Modification of Spatial and Temporal Gains of Stimulated Brillouin and Raman Scattering by Polarization Smoothing

J. Fuchs,[1] C. Labaune,[1] S. Depierreux,[1] H. A. Baldis,[2] and A. Michard[1]

[1]*Laboratoire pour l'Utilisation des Lasers Intenses, UMR 7605 CNRS-École Polytechnique-CEA-Université Paris VI, École Polytechnique, 91128 Palaiseau Cedex, France*

[2]*Institute for Laser Science and Applications (ILSA), Lawrence Livermore National Laboratory, Livermore, California 94550*

(Received 7 December 1999)

Significant reductions of stimulated Brillouin (SBS) and Raman (SRS) scattering are measured by adding polarization smoothing (PS) to a random phase plate smoothed beam. The associated plasma waves, as measured by Thomson scattering, are spatially and temporally modified and reveal that the interplay between SBS and SRS has to be taken into account to understand the effect of the smoothing. The results also support the numerical simulations [S. Hüller *et al.,* Phys. Plasmas **5**, 2706 (1998); R. Berger *et al.,* Phys. Plasmas **6**, 1043 (1999)] predicting a reduction of self-focusing with PS, resulting in a decrease of the maximum laser intensity and consequently of SBS and SRS gains.

PACS numbers: 52.40.Nk, 52.35.Fp, 52.35.Mw, 52.70.Kz

Wave front aberrations induced by high amplification of laser beams lead to inhomogeneous focal spots with undesirable hot spots whose intensity can be much greater than the average beam intensity. In laser-plasma interactions, those hot spots can have severe effects such as breaking the stringent irradiation uniformity level required in both direct and indirect approaches to inertial confinement fusion (ICF). They also favor the growth of stimulated Brillouin (SBS) and Raman (SRS) scattering [1], leading to the scattering of a significant portion of the incoming laser light and thus preventing an efficient coupling of the laser light with the target. Hot spots are also prone to self-focus, due to the combined action of the thermal pressure and the ponderomotive force [1]. Such a phenomenon further reduces the focal spot uniformity and enhances SBS and SRS. All these detrimental processes, of concern for ICF, become more crucial in the prospect of the achievement of the megajoule-scale laser facilities in France (Laser MégaJoule or LMJ) [2] and in the USA (National Ignition Facility or NIF) [3].

In this context it is particularly important to experimentally investigate the effect of the techniques that have been proposed to control parametric instabilities by spatial and temporal smoothing of the laser beam intensity distribution. Reduction of self-focusing, SBS, and SRS have been observed using random phase plate (RPP) [4] or smoothing by spectral dispersion [5,6], but even then, significant scattering levels have been observed in plasma approaching the NIF or LMJ conditions [7]. In addition to the previous techniques, polarization smoothing (PS) consists in dividing the light power into two beams with crossed polarizations and slightly shifted focal spots [8]. With PS added to RPP, a strong reduction of the self-focusing in the high intensity speckles has been numerically observed [9]. By lowering the power in these high intensity speckles which contribute the most to SBS and SRS, this control of self-focusing has been shown to reduce the gains of these instabilities [10,11].

In this Letter, we present the first results showing the reduction as well as temporal and spatial modifications of SBS and SRS in underdense preformed plasmas when adding PS to an RPP interaction beam. First, we observe remarkable reduction of SBS and SRS reflectivities in backward direction, by up to a factor of 10 for SBS and 3 for SRS. Consistently, we measure a reduction of the amplitudes of the associated ion acoustic waves (IAWs) and electron plasma waves (EPWs). Second, simultaneous Thomson scattering from both IAWs and EPWs shows that an earlier vanishing of the IAWs leads to an earlier emergence of the EPWs. This suggests that the competition among the instabilities can act to lower the effect the PS technique has on SRS. Third, the location of IAWs, which is in the front part of the density profile, is seen closer to the summit with RPP + PS, in agreement with a smaller blueshift of the backscattered SBS light. This feature supports the interpretation of reduced self-focusing induced by PS.

The experiments are performed with five beams of the LULI (Laboratoire pour l'Utilisation des Lasers Intenses) laser facility. All beams are in the horizontal plane with 600 ps full width at half maximum (FWHM) Gaussian pulses. The targets are 380 μm diameter free-standing CH disks of thickness 1.2 μm. These are completely exploded by two 526 nm counterpropagating beams with RPP focal spots larger than the target. The plasma is heated by a third, identical beam, delayed by 0.5 ns with respect to the first two. The $\lambda_0 = 1.053$ μm interaction beam is focused with an $f = 500$ mm, $f/6$ lens through an RPP (a circular array of 2 mm elements) along the principal axis of the plasma expansion and delayed by 1.4 ns with respect to the plasma formation pulses. Its focal spot diameter is 320 μm FWHM, leading to a peak average intensity $I_0 = 10^{14}$ W/cm^2. The transverse and longitudinal sizes of the speckles are 7.5 and 290 μm, respectively.

A 351 nm Thomson scattering probe, synchronous with the interaction beam, is focused through an RPP with

elongated elements to form a focal region 100 μm by 1 mm along the axis of the interaction beam, thus allowing us to image the location of the waves over the whole interaction length. We preferentially collect the Thomson scattered light from IAWs and EPWs associated with backward SBS and SRS. The SBS backscattered light collected in the focusing optics is measured in energy and spectrum, with temporal resolution. The SRS backscattered light is measured in energy with a cold Au-Ge detector with a flat response in the spectral range, limited by optical filters, between 1.2 and 1.95 μm.

Time-resolved spectra of thermal Thomson scattering recorded in the vertical direction (where there is no contribution from pumped waves by the interaction beam) give electron temperatures of 0.5–0.7 keV during the interaction pulse. This diagnostic also gives a measurement of the expanding plasma flow velocity along the laser axis. The temporal evolution of the electron density at specific locations in the plasma and the electron density profiles along the laser axis are inferred using Thomson scattered spectra off SRS-EPWs [12]. The electron density at the peak of the plasma profile evolves from $0.45n_c$ to $0.05n_c$ during the interaction beam (where $n_c = 1 \times 10^{21}$ cm^{-3} is the critical electron density for λ_0). The typical scale length of the parabolic profile of the plasma is 700 μm.

As illustrated in Fig. 1, polarization smoothing of the interaction beam is obtained by propagating the beam through a wedged birefringent crystal (type II KDP, potassium-dihydrogen-phosphate) with its polarization at 45° from both the ordinary and the extraordinary axis of the crystal. At the output, the incident beam is thus split into two angularly separated beams with equal power and orthogonal polarizations. The two waves are propagated through an RPP and then focused. In the focal plane, the two speckle patterns do not interfere since the waves are incoherent by polarization; they simply add up in intensity with a spatial separation ~9 μm in our case. As this value is larger than the transverse size of the speckles, the two beams can be considered as uncorrelated.

Figure 2 shows the SBS and SRS reflectivities measured using RPP and RPP + PS smoothing techniques as a function of the average interaction beam intensity. Both reflectivities grow with intensity, for the entire explored domain, with no clear sign of overall saturation. With PS added and for all intensities, the results clearly indicate a strong and constant reduction in the backscattered energy, by a factor of ~10 for SBS and ~3 for SRS. It is worth noticing that the same conclusions can be drawn when we use a $f/3$ focusing optics or different target materials like aluminum or carbon-deuterium targets.

Beyond the measurement of backscattered energies, it is interesting to observe the detailed modifications induced on the SBS and SRS instabilities by PS. This is achieved using the imaging diagnostic that allows us to simultaneously observe the light scattered off IAWs and EPWs. Figure 3 shows typical spatial and temporal evolution of IAWs and EPWs for both RPP [Fig. 3(a)] and RPP + PS [Fig. 3(b)] beams. As observed in previous experiments [13], the two types of waves are temporally anticorrelated and grow over overlapping regions in the front part of the plasma. In the following, we concentrate on the modification of these spatial and temporal behaviors with PS.

One can see [Fig. 3(b)] that IAWs are much more modified by PS than EPWs, which corroborates the backscattered energy measurements shown in Fig. 2. With PS added and for all laser intensities, not only the amplitude of IAWs is strongly reduced, but they also grow closer to the top of the density profile [see Fig. 3(c)] and last for a shorter time. They are shortened from 250 to 150 ps (FWHM) with PS.

The most interesting result from this diagnostic is the corresponding modification of the temporal behavior of EPWs with PS. In both Figs. 3(a) and 3(b), we observe that EPWs do not grow early in the laser pulse, although the SRS threshold is reached. This is probably due to some inhibition of the EPWs induced by ion acoustic fluctuations associated with SBS [14]. However, we notice in Fig. 3(b) that a reduction of these ion fluctuations by PS let the EPWs grow earlier, by ~180 ps, and more rapidly than in the RPP only case. This is one more sign that a decrease of the amplitude of IAWs directly affects the temporal growth of EPWs and modifies the temporal interplay between the two instabilities. It is consistent with the modification of the competition between SBS and SRS, which has been observed under beam crossing irradiation

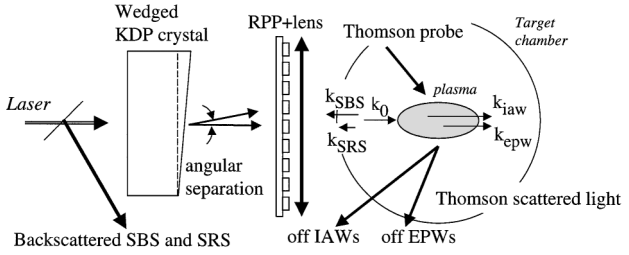

FIG. 1. Polarization-smoothing arrangement (the angular separation between the two orthogonally polarized beams is grossly exaggerated) and scheme of the diagnostics.

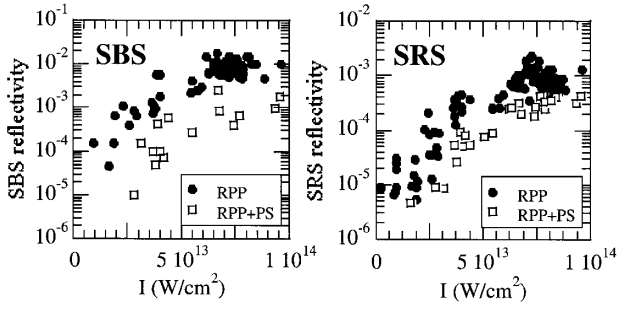

FIG. 2. SBS and SRS reflectivities as a function of the average interaction beam intensity. RPP + PS with respect to RPP only reduces backscatter from a factor of 10 (SBS) to 3 (SRS).

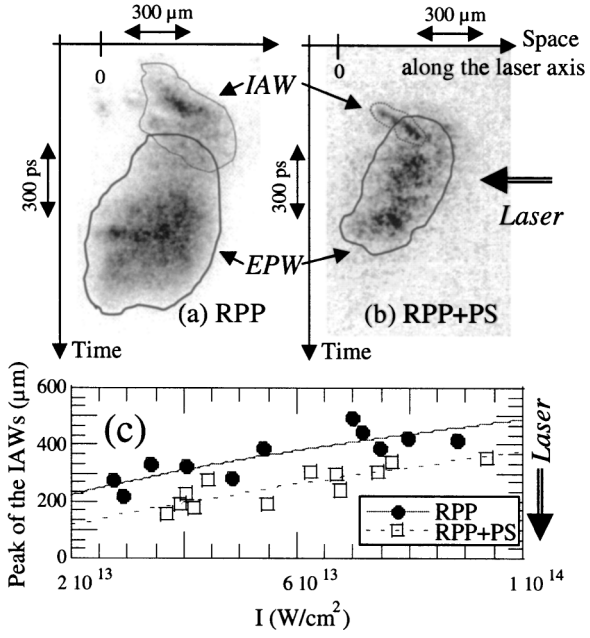

FIG. 3. (a) Image of Thomson scattered light off both SBS-IAWs and SRS-EPWs as a function of time and space. The laser comes from the right with an intensity of 8×10^{13} W/cm^2. RPP is used in this case. Position 0 corresponds to the initial target location. The thin dashed (solid) line corresponds to a contour at one-tenth of the peak IAW (EPW) intensity. (b) The same as (a) but for an RPP + PS beam. The top of the two images corresponds to the same time with respect to the plasma creation. (c) Peak amplitude location, as measured in the images, of the scattered light off SBS-IAWs as a function of the beam intensity for both RPP and RPP + PS beams.

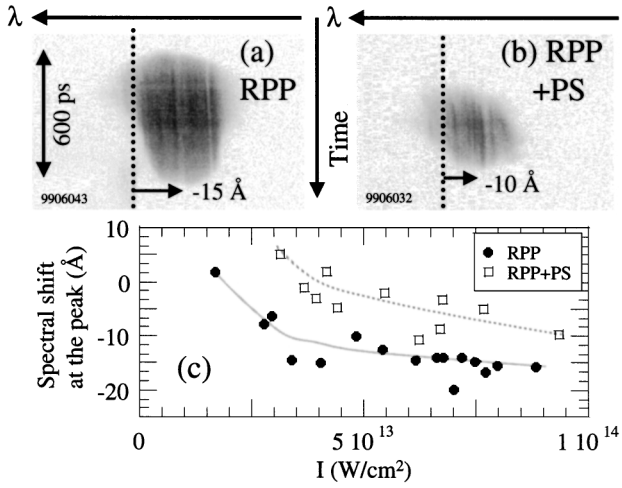

FIG. 4. (a) Time-resolved SBS backscatter spectrum at an intensity of 9×10^{13} W/cm^2 (RPP beam). The dotted line corresponds to the incident laser wavelength of 1.053 μm, but the absolute timing for the two images is different. In agreement with the direct observation of SBS-IAWs of Fig. 3, the signal is emitted during the first half of the laser pulse. (b) The same as (a) but for an RPP + PS beam. The same filtering is used for both images. (c) Measured average spectral shift of the backscattered spectrum as a function of the laser intensity for both RPP and RPP + PS beams.

[15] and attributed to nonlinear enhancement of the IAW damping rate [16]. This interplay may suggest an explanation for the fact that we observe a smaller overall reduction for SRS than for SBS. Indeed, in the case of SRS, two effects may act in opposite ways: (i) the inhibited growth of the IAWs induced by PS allows EPWs to grow stronger and, at the same time, (ii) the reduced power in the high intensity speckles caused by PS decreases the growth of the EPWs.

The time-resolved spectra of the SBS backscattered light also exhibit strong differences between the RPP and RPP + PS cases. As shown in Figs. 4(a) and 4(b), the spectra are smooth and broad in both cases. They exhibit large blueshifts (with respect to the incident laser wavelength) that increase with the laser intensity. However, this shift is less important in the RPP + PS case. This difference in the blueshift remains for all laser intensities as can be seen in Fig. 4(c). Using the dispersion relation for IAW, the SBS k-matching condition and the plasma flow velocity measured by thermal Thomson scattering [u(m/s) $\sim 700(z(\mu\text{m}) + 250)$], we find that, for all laser energies, the spectral blueshift of the backscattered SBS light is consistent with the location of the IAWs as measured with the imaging diagnostic (see Fig. 3). Thus, Fig. 4(c) confirms the result displayed in Fig. 3(c): SBS-IAWs grow closer to the top of the profile in the RPP + PS case. For all the measurements, we verify, in the RPP case without PS, that we obtain identical results when rotating the polarization of the interaction beam. Thus we assess that the effects we observe in the RPP + PS case, with respect to RPP only, are not due to a different polarization of the beam.

The change of the laser intensity distribution in the focal volume induced by PS is likely to be the source of the SBS and SRS gain modifications observed here. It can be easily shown [9,17] that the intensity contrast of the focal spot pattern is reduced from 1 to $1/\sqrt{2}$ from RPP to RPP + PS, and that the fraction of the beam intensity above nI_0 (I_0 being the averaged peak intensity) goes from $(1 + n)\exp(-n)$ for RPP to $(1 + 2n + 1n^2)\exp(-2n)$ for RPP + PS, indicating that the fraction of the laser power in the high intensity speckles (the more prone to self-focus) is reduced. It also has been shown in recent work [18], using a statistical approach, that the reflectivity levels and the localization of the waves observed in experiments using RPP could be explained by scattering in a few self-focused intense hot spots.

The strong reduction of self-focusing induced by PS has been numerically shown [9,10]. The threshold power for ponderomotive self-focusing is $P_c(\text{MW}) \approx 32T_e(\text{keV})n_c/n_e\sqrt{1 - n_e/n_c}$ (see, e.g., [11]). In our conditions, for each speckle, this corresponds to a threshold (in intensity) of 5×10^{14} W/cm^2. From statistical theory [19], we know that the mean value of the maximum intensity in the hot spots is $11 \times I_0 \sim 10^{15}$ W/cm^2 (for

higher intensity values the expected number of speckles is less than 1). This implies that, with RPP only, these high intensity hot spots are above the self-focusing threshold. However, with PS added, the intensity in the most intense hot spots is lowered by a factor of 2 [19], bringing it down to 5×10^{14} W/cm^2, where self-focusing becomes marginally unstable. This could explain the observed impact PS has here on parametric instabilities. Numerical studies [11] with parameters close to ours exhibit the same trends as the ones we observe: significantly lower SBS reflectivities and higher SBS threshold for RPP + PS with respect to RPP.

The changes in the localization of the IAWs and in the SBS blueshift are also consistent with this frame of reduced self-focusing when PS is added. Indeed, concerning the localization of the SBS-IAWs in the front part of the profile (consistent with the backscatter SBS blueshift) and its drift towards the incoming laser with increasing laser intensity, one of the most likely explanations is the occurrence of self-focusing of the beam in the front part of the density profile. Spreading of the light at the output of the self-focused filaments can lead to a decrease of the intensity at higher densities in the profile and consequently to a reduction of the growth of the waves there. It is worth noticing that the same explanation of reduced self-focusing was proposed for experiments using temporal smoothing techniques [6], where a reduction of the SBS blueshift has been reported. However the picture can be more complex since (i) the speckle distributions are calculated in vacuum and can be significantly modified in the plasma [9,10] and (ii) SBS and SRS compete [13], not only between themselves but also with self-focusing. More complete simulations using the numerical simulation code F3D [10] are under way and will bring a better understanding of these results.

In summary, we have experimentally demonstrated the effectiveness of the PS technique in reducing the growth of SBS and SRS in an underdense plasma. By instantaneously reducing the residual small-scale inhomogeneity left in the RPP speckle pattern, PS succeeds in lowering the power in the fast self-focusing hot spots. The reduction in self-focusing and growth of the instabilities could be made even greater by combining PS to the temporal smoothing complementary technique. These results have obvious important implications in the context of ICF.

The authors gratefully acknowledge the support of the technical groups of LULI. We are grateful to R. Berger, E. Lefebvre, and G. Bonnaud for useful discussions. We also thank J. L. Miquel at CEA/BIII for the loan of a streak camera. This work was partially supported under the auspices of the U.S. Department of Energy by the Lawrence Livermore National Laboratory under Contract No. W-7405-ENG-48. Part of this support was provided through the LLNL-LDRD program under the Institute for Laser Science and Applications.

[1] W. L. Kruer, *The Physics of Laser Plasma Interactions* (Addison Wesley, New York, 1988).
[2] M. André, *Inertial Fusion Science and Applications* (Elsevier Gauthier Villars, Paris, 2000), p. 32.
[3] T. Dittrich *et al.,* Phys. Plasmas **6**, 2164 (1999).
[4] Y. Kato *et al.,* Phys. Rev. Lett. **53**, 1057 (1984); C. Labaune *et al.,* Phys. Fluids B **4**, 2224 (1992).
[5] S. Skupsky *et al.,* J. Appl. Phys. **66**, 3456 (1989); O. Willi *et al.,* Phys. Fluids B **2**, 1318 (1990); W. Seka *et al.,* Phys. Fluids B **4**, 2232 (1992).
[6] J. D. Moody *et al.,* Phys. Plasmas **2**, 4285 (1995).
[7] R. Kirkwood *et al.,* Phys. Plasmas **4**, 1800 (1997); B. McGowan *et al.,* Phys. Plasmas **3**, 2029 (1996).
[8] LLE Review **45**, 1 (1990). Available from the National Technical Information Services, U.S. Department of Commerce, 5285 Port Royal Road, Springfield, VA 22161; K. Tsubakimoto *et al.,* Opt. Commun. **91**, 9 (1992).
[9] E. Lefebvre *et al.,* Phys. Plasmas **5**, 2701 (1998).
[10] R. Berger *et al.,* Phys. Plasmas **6**, 1043 (1999).
[11] S. Hüller *et al.,* Phys. Plasmas **5**, 2706 (1998).
[12] H. Baldis *et al.,* Rev. Sci. Instrum. **67**, 451 (1996).
[13] C. Labaune *et al.,* Phys. Plasmas **4**, 423 (1997).
[14] W. Rozmus *et al.,* Phys. Fluids **26**, 1071 (1983); J. Heikkinen *et al.,* Phys. Fluids **29**, 1291 (1986); G. Bonnaud, Laser Part. Beams **5**, 101 (1987).
[15] C. Labaune *et al.,* Phys. Rev. Lett. **82**, 3613 (1999).
[16] B. Cohen *et al.,* Phys. Plasmas **5**, 3402 (1998).
[17] J. Goodman, in *Laser Speckle and Related Phenomena,* edited by J. Dainty (Springer-Verlag, Berlin, 1984).
[18] V. Tikhonchuk *et al.,* Phys. Plasmas **3**, 3777 (1996); H. Baldis *et al.,* Phys. Rev. Lett. **80**, 1900 (1998).
[19] J. Garnier *et al.,* J. Mod. Opt. **46**, 1213 (1999).